The Astrophysical Journal, 671: L153–L156, 2007 December 20

A SEARCH FOR *ortho*-BENZYNE (*o*-C_6H_4) IN CRL 618

Susanna L. Widicus Weaver,[1] Anthony J. Remijan,[2] Robert J. McMahon,[3] and Benjamin J. McCall[1]

Received 2007 September 5; accepted 2007 November 1; published 2007 November 30

ABSTRACT

Polycyclic aromatic hydrocarbons (PAHs) have been proposed as potential carriers of the unidentified infrared bands (UIRs) and the diffuse interstellar bands (DIBs). PAHs are not likely to form by gas-phase or solid-state interstellar chemistry, but rather might be produced in the outflows of carbon-rich evolved stars. PAHs could form from acetylene addition to the phenyl radical (C_6H_5), which is closely chemically related to benzene (C_6H_6) and *ortho*-benzyne (*o*-C_6H_4). To date, circumstellar chemical models have been limited to only a partial treatment of benzene-related chemistry, and so the expected abundances of these species are uncertain. A detection of benzene has been reported in the envelope of the proto–planetary nebula (PPN) CRL 618, but no other benzene-related species has been detected in this or any other source. The spectrum of *o*-C_6H_4 is significantly simpler and stronger than that of C_6H_5, and so we conducted deep Ku-, K-, and Q-band searches for *o*-C_6H_4 with the Green Bank Telescope. No transitions were detected, but an upper limit on the column density of 8.4×10^{13} cm^{-2} has been determined. This limit can be used to constrain chemical models of PPNe, and this study illustrates the need for complete revision of these models to include the full set of benzene-related chemistry.

Subject headings: astrochemistry — circumstellar matter — radio lines: stars — stars: individual (CRL 618)

1. INTRODUCTION

Polycyclic aromatic hydrocarbons (PAHs) are large molecules with carbon atoms arranged in five- or six-membered rings and are thought to form from smaller carbon ring molecules such as benzene (C_6H_6) and its derivatives. PAHs are very stable against photodissociation, and so could be present in interstellar and/or circumstellar environments. The unidentified infrared bands (UIRs) occur at frequencies characteristic of aromatic molecules, and so PAHs have been suggested as potential UIR carriers. Likewise, PAHs have been proposed as carriers of the diffuse interstellar bands (DIBs). We refer the reader to a recent review of the DIB problem by Sarre (2006) and references therein for a discussion of PAHs and their relation to the UIRs and DIBs. Significant laboratory spectroscopic work has been dedicated to PAHs and other benzene-related species to support astronomical observations, yet none of these species has been unambiguously detected in space. Only benzene has been tentatively detected toward the proto–planetary nebula (PPN) CRL 618 (Cernicharo et al. 2001a). One vibrational band of benzene was observed, and a column density of 5×10^{15} cm^{-2} and a kinetic temperature of 200 K were determined.

CRL 618 is an evolved PPN with a central B0 star and an ultracompact H II region surrounded by a carbon-rich molecular envelope (Cernicharo et al. 2001b; Sánchez Contreras & Sahai 2004). This source has optical high-velocity bipolar outflows (Trammell 2000) in addition to a low-velocity expanding torus of molecular emission (Sánchez Contreras & Sahai 2004). CRL 618 has a rich molecular inventory including a variety of hydrocarbons (see Pardo et al. 2007 and references therein), but searches for biologically important molecules have provided only upper limits (Remijan et al. 2005).

Very few observational constraints have been placed on the chemical and physical properties of PPNe, especially regarding benzene-related chemistry. Observational studies of the simplest benzene derivatives are the essential first steps to understanding the formation of PAHs in PPNe. The carbon-rich nature of CRL 618, coupled with the benzene detection, makes it an excellent target for initial benzene derivative searches. We have therefore conducted a search for the benzene derivative *ortho*-benzyne (*o*-C_6H_4) in CRL 618 with the Green Bank Telescope (GBT) Ku-, K-, and Q-band receivers. An overview of circumstellar benzene-related chemistry, details of the observations, the results of our search, and a discussion of these results are presented below.

2. BENZENE-RELATED CIRCUMSTELLAR CHEMISTRY

PAHs have long been thought to be produced in carbon-star outflows, as it seems unlikely that such large molecules could be produced by gas-phase or grain-assisted chemistry within the interstellar medium. Although the PPN phase of stellar evolution is typically very short, lasting only about 10,000 years, the chemistry that takes place in the envelope of the post–asymptotic giant branch (AGB) star leads to the formation of complex hydrocarbons. PPN chemistry is steeply dependent on density because circumstellar material undergoes energetic processing, and formation mechanisms for large molecules are likely a combination of radical-molecule and ion-molecule reactions. This is in contrast to low-density interstellar chemistry that is almost exclusively driven by ion-molecule reactions. Both radical-molecule and ion-molecule reactions can lead to the formation of benzene and related species, and such benzene formation mechanisms have been included in PPN models (Redman et al. 2003; Woods et al. 2003). However, no PPN model includes both the radical- and ion-based benzene reaction networks. This striking deficiency in PPN models makes interpretation of observational results quite difficult, and the radical- and ion-based chemical mechanisms must be considered separately until more complete PPN models are developed.

The torus of a PPN is a high-energy, high-density environment, and the chemistry is expected to be similar to that observed in combustion (Frenklach & Feigelson 1989). Radical-based mechanisms based on combustion chemistry have been proposed for benzene and PAH formation in the circumstellar

[1] Departments of Chemistry and Astronomy, University of Illinois at Urbana-Champaign, Urbana, IL 61801; slww@uiuc.edu, bjmccall@uiuc.edu.
[2] National Radio Astronomy Observatory, Charlottesville, VA 22903; aremijan@nrao.edu.
[3] Department of Chemistry, University of Wisconsin–Madison, Madison, WI 53706; mcmahon@chem.wisc.edu.

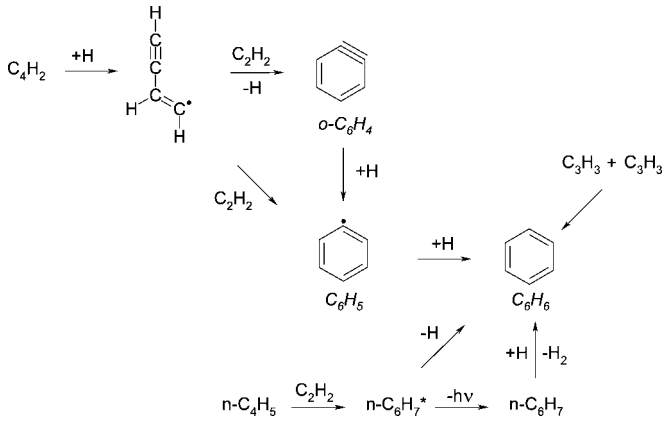

FIG. 1.—Radical-based reaction scheme for PPNe benzene chemistry based on Frenklach & Feigelson (1989).

shells of AGB stars (Cherchneff et al. 1992), and a subset of these reactions was also used to model the chemistry of clumps during PN evolution (Redman et al. 2003). A summary of radical-driven benzene chemistry is shown in Figure 1. Here, hydrocarbon radicals react with acetylene (C_2H_2), and ring-closure forms *o*-C_6H_4. Additional reactions lead to the phenyl radical (C_6H_5) and benzene. Other routes to benzene include either reaction of two C_3H_3 radicals or, alternatively, the formation of straight-chain energetic C_6H_7 (n-$C_6H_7^*$), which can then undergo ring-closure.

As a PPN evolves and its surrounding gas expands, the density decreases and the material in the circumstellar envelope is subjected to photoprocessing from the central star, leading to ion-molecule chemistry. An ion-molecule benzene formation mechanism has been proposed for PPNe (Woods et al. 2003), and a summary of this mechanism is shown in Figure 2. In this network, hydrocarbon ions react with acetylene, and ring closure forms $C_6H_5^+$. Additional hydrogenation and/or electron recombination leads to *o*-C_6H_4, *c*-$C_6H_7^+$, and ultimately C_6H_6. It should be noted that the original PPN model investigated only the primary route to benzene shown in Figure 2 and did not include the *o*-C_6H_4 formation reaction (Woods et al. 2003).

One of the benzene derivatives formed in these reactions, C_6H_5, is a suggested precursor to PAHs in circumstellar environments (Frenklach & Feigelson 1989; Cherchneff et al. 1992). As is illustrated in Figure 3, C_6H_5 can undergo a series of radical-molecule reactions involving acetylene to produce a

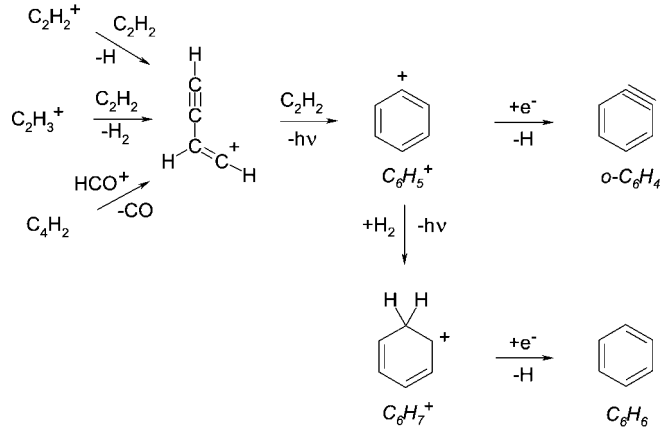

FIG. 2.—Ion-based chemical scheme for PPNe benzene chemistry based on Woods et al. (2003).

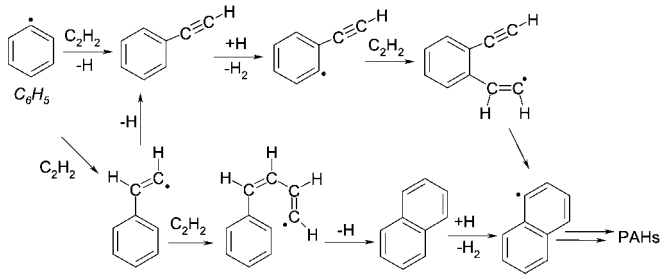

FIG. 3.—Potential PAH formation routes in circumstellar shells (Frenklach & Feigelson 1989; Cherchneff et al. 1992).

naphthalene-like species ($C_{10}H_8$) via ring-closure. Subsequent reactions of this nature can lead to larger PAHs.

Studies of other high-energy environments indicate that C_6H_5 and *o*-C_6H_4 may well coexist with benzene in CRL 618 if circumstellar chemistry is similar to combustion or plasma chemistry. The reaction network of Frenklach & Feigelson (1989) is based on soot production mechanisms in hydrocarbon flames, and theoretical studies show that benzene unimolecular decomposition leads to C_6H_5 and *o*-C_6H_4 during combustion (Mebel et al. 2001). Benzene electrical discharges also produce C_6H_5 and *o*-C_6H_4 (McMahon et al. 2003). There are no reliable predictions of C_6H_6, C_6H_5, and *o*-C_6H_4 abundances in PPNe because of the partial treatment of their chemistry in models, but observations of C_6H_5 and *o*-C_6H_4 would provide important limits for future modeling studies. We therefore began a search for these species in CRL 618.

C_6H_6 has no permanent dipole moment and can therefore only be studied in the infrared, but both C_6H_5 and *o*-C_6H_4 can be probed by radioastronomical techniques. The rotational spectra of *o*-C_6H_4 and C_6H_5 have been obtained in the laboratory (Brown et al. 1986; Robertson et al. 2003; Kukolich et al. 2003; McMahon et al. 2003). Both species are carbon ring, planar, near-oblate asymmetric rotors with C_{2v} symmetry along their *b* inertial axes. The calculated dipole moment of *o*-C_6H_4 is 1.38 D (Kraka & Cremer 1993) and that of C_6H_5 is 0.9 D (McMahon et al. 2003). The unpaired electron in C_6H_5 leads to hyperfine splitting of the lower rotational states (McMahon et al. 2003), and so there are many rotational transitions to sample observationally. However, the larger di-

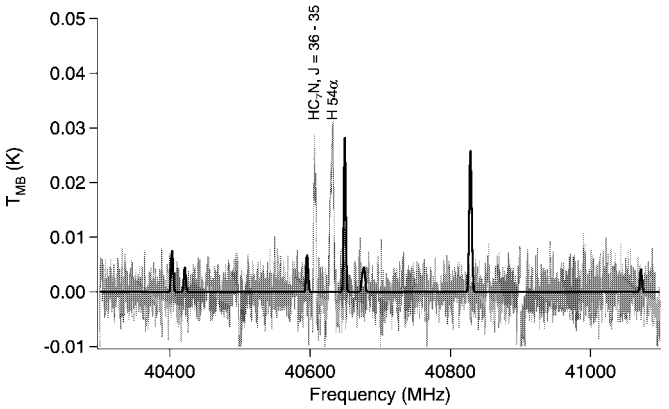

FIG. 4.—Observed CRL 618 Q-band spectrum (*gray*) overlaid with a simulation of the *o*-C_6H_4 spectrum (*black*) at a column density of 10^{16} cm^{-2}, a rotational temperature of 200 K, and a source size of 10″. The observed spectrum is comprised of four 200 MHz windows and has been additionally smoothed to a resolution of 200 kHz for further clarity. The features at 40500 and 40900 MHz arise from noise at the edges of the spectral windows.

TABLE 1
SUMMARY OF o-C_6H_4 OBSERVATIONS TOWARD CRL 618

$J'_{K'_a,K'_c}$–$J''_{K''_a,K''_c}$	ν (MHz)	Ag_u (s^{-1})	E_u (K)	T_{MB} (mK)	η	N_T Upper Limit (cm^{-2})
$4_{2,2}$–$4_{1,3}$	13250.8230	6.08×10^{-7}	5.28	1.48	0.92	3.47×10^{15}
$3_{3,1}$–$3_{2,2}$	13680.0050	3.59×10^{-7}	3.70	1.76	0.92	6.87×10^{15}
$6_{5,1}$–$6_{4,2}$	14608.9021	1.28×10^{-6}	12.37	1.45	0.91	1.59×10^{15}
$3_{1,2}$–$3_{0,3}$	14619.6969	2.40×10^{-7}	2.96	1.45	0.91	8.22×10^{15}
$2_{0,2}$–$1_{1,1}$	14753.9974	4.23×10^{-7}	1.19	1.45	0.91	4.62×10^{15}
$3_{0,3}$–$2_{1,2}$	21770.7375	1.60×10^{-6}	2.26	2.47	0.86	1.79×10^{15}
$4_{2,3}$–$4_{1,4}$	21963.3591	7.93×10^{-7}	4.67	2.47	0.86	3.63×10^{15}
$11_{8,3}$–$11_{7,4}$	22142.0552	5.35×10^{-6}	37.44	2.18	0.85	5.28×10^{14}
$9_{5,4}$–$9_{4,5}$	22143.1890	4.10×10^{-6}	24.25	2.18	0.85	6.60×10^{14}
$3_{1,3}$–$2_{0,2}$	22216.3288	2.88×10^{-6}	2.26	2.18	0.85	8.72×10^{14}
$7_{5,3}$–$7_{4,4}$	23578.9636	5.35×10^{-6}	15.55	2.51	0.84	5.56×10^{14}
$2_{2,1}$–$1_{1,0}$	24109.5097	1.40×10^{-6}	1.77	1.76	0.84	1.42×10^{15}
$3_{1,2}$–$2_{2,1}$	24842.4030	8.22×10^{-7}	2.96	2.13	0.83	2.90×10^{15}
$8_{2,6}$–$8_{1,7}$	40403.3815	1.64×10^{-5}	16.25	6.42	0.64	4.19×10^{14}
$8_{3,6}$–$8_{2,7}$	40421.4144	9.83×10^{-6}	16.25	6.42	0.64	6.98×10^{14}
$5_{1,4}$–$4_{2,3}$	40595.9260	1.40×10^{-5}	6.62	5.92	0.63	4.37×10^{14}
$22_{13,9}$–$22_{12,10}$	40649.5538	1.13×10^{-4}	137.89	5.92	0.63	8.40×10^{13}
$7_{1,6}$–$7_{0,7}$	40674.4124	5.21×10^{-6}	11.45	5.92	0.63	1.19×10^{15}
$7_{2,6}$–$7_{1,7}$	40677.1133	8.69×10^{-6}	11.45	5.92	0.63	7.16×10^{14}
$6_{0,6}$–$5_{1,5}$	40828.1686	4.05×10^{-5}	7.23	6.21	0.63	1.59×10^{14}
$6_{1,6}$–$5_{0,5}$	40829.9929	2.43×10^{-5}	7.23	6.21	0.63	2.64×10^{14}
$3_{3,0}$–$2_{2,1}$	41071.9441	8.57×10^{-6}	3.74	9.40	0.63	1.12×10^{15}

pole moment coupled with the lack of hyperfine splitting yields much stronger lines for o-C_6H_4 and makes this species a more likely candidate for detection if the abundances are similar.

3. OBSERVATIONS

Observations of o-C_6H_4 were conducted with the NRAO[4] 100 m Robert C. Byrd GBT between 2006 September 4 and 2007 January 28 using the Ku-band (12–15.4 GHz), K-band (18–22.5 and 22–26.5 GHz), and Q-band (40–48 GHz) receivers. The eight intermediate-frequency (IF), 200 MHz, three-level GBT spectrometer configuration mode was used, providing four 200 MHz frequency bands with a channel separation of 24.4 kHz in two polarizations. The assumed CRL 618 J2000.0 pointing position and LSR source velocity were $\alpha = 04^h42^m53.7^s$, $\delta = +36°06'53.0''$ and -27.5 km s^{-1}, respectively. Data were acquired in the OFF-ON position-switching mode. A scan included 2 minute integrations for each position beginning with the OFF-source position, which was located $60'$ east in azimuth of the ON-source position. Antenna temperatures with estimated 20% uncertainties were recorded on the T_A^* scale (Ulich & Haas 1976). The GBT half-power beamwidths are given by $\theta_b = 740''/\nu$(GHz). Dynamic pointing and focusing corrections were applied and observations of the quasar 0359+509 were used to adjust the zero points every 2 hours or less. Observations from multiple nights and both polarizations were averaged for each frequency window, and the data were Hanning smoothed over three channels with the GBDish data reduction program. The resulting Q-band spectrum is shown in Figure 4.

Table 1 lists the o-C_6H_4 rotational transitions in the observed frequency windows. The transition quantum numbers, transition rest frequency (ν), the Einstein A coefficient of the transition times the upper state degeneracy (Ag_u), the energy of the upper level (E_u), the observed 1σ rms level (T_{MB}), and the beam efficiency (η) are listed in the first six columns. The transition frequencies and intensities are from the Cologne Database for Molecular Spectroscopy (Müller et al. 2005). The d.rms routine in GBDish was used to calculate the rms level in the T_A^* scale for each spectral window. The rms level is equal to the standard deviation of the noise in a line-free region and was calculated after the Hanning smoothing was applied. These values were then converted to the T_{MB} scale by the relationship $T_{MB} = T_A^*/\eta$. The value of η was derived from a fit to the Ruze (1966) formulation, as is outlined in equation (2) of Hollis et al. (2007).

4. RESULTS AND DISCUSSION

No spectral features associated with o-C_6H_4 were detected during this search, and there are no unidentified spectral features in any passband. Figure 4 shows a plot of the observed CRL 618 Q-band spectrum overlaid by a predicted o-C_6H_4 spectrum at a column density of 10^{16} cm^{-2}, a rotational temperature of 200 K, and a source size of $10''$. If these parameters are representative of o-C_6H_4, the blended $6_{0,6}$–$5_{1,5}$ and $6_{1,6}$–$5_{0,5}$ transitions at 40828.1686 and 40829.9929 MHz, respectively, should have been easily detected at the 30 mK level.

The rms levels reached during the observations allow calculation of the o-C_6H_4 column density upper limit in CRL 618, and the 3σ upper limits determined from each observed transition are presented in Table 1. These column density upper limits were calculated using the following expression, adapted from equation (1) of Nummelin et al. (1998):

$$N_T = \int_{-\infty}^{\infty} T_b dv \, \frac{8\pi k \nu^2}{hc^3} \, \frac{Q(T_{\rm rot})}{Ag_u} \exp\left(E_u/kT_{\rm rot}\right), \qquad (1)$$

where N_T is the beam averaged total column density, $\int_{-\infty}^{\infty} T_b dv$ is the transition integrated intensity, $Q(T_{\rm rot})$ is the rotational partition function, and $T_{\rm rot}$ is the molecular rotational temperature. Since no lines were observed, the integrated intensity was approximated as that of a line with a peak intensity at the 3σ rms level, $T_{\rm rms}$, and an assumed line width Δv. The value of $T_{\rm rms}$ was determined by $T_{\rm rms} = 3T_{MB}/\sqrt{n}$, where n is the number of channels across the line width Δv. The $1/\sqrt{n}$ factor does not include a complete statistical treatment of the assumed Gaussian line shape, but it does approximate the overestimation of the rms level from spectral oversampling. Examination of previously reported upper limit calculations indicates that, in many cases, this factor is either neglected entirely, or at the very least not discussed explicitly. We find this to be a gross omission for instruments such as the GBT spectrometer, where the channel width is often significantly smaller than the line width. From the $T_{\rm rms}$ values, correction for beam dilution gave T_b through the expression $T_b = T_{\rm rms}/B$, where the beam filling factor B was calculated from the source size θ_s and the beam size θ_b by the relationship $B = \theta_s^2/(\theta_s^2 + \theta_b^2)$. The integrated intensity was then approximated as $\int_{-\infty}^{\infty} T_b dv = 1.064 T_b \Delta v$, where the 1.064 factor arises from the assumed Gaussian line shape. We have included this factor for completeness, although it is likely minimal compared to the uncertainty in T_b.

The calculated 3σ o-C_6H_4 upper limits for CRL 618 are presented in Table 1. These calculations required assumptions for the values of $T_{\rm rot}$, Δv, and θ_s. The line width was assumed to be that observed for other identified lines, 10 km s^{-1}. Determination of an appropriate temperature and source size was less straightforward, as there is much discrepancy in the literature regarding these values. The kinetic temperature derived

[4] The National Radio Astronomy Observatory is a facility of the National Science Foundation, operated under cooperative agreement by Associated Universities, Inc.

for benzene is 200 K (Cernicharo et al. 2001a), but an IRAM 30 m millimeter line survey indicates temperatures of 250–275 K for the torus and 30 K for the circumstellar shell (Pardo et al. 2007). It is expected that *o*-C_6H_4 would have very similar physical properties to those of benzene in this source, and so a temperature of 200 K was assumed for the upper limit calculations.

Similarly, there is a range in the observationally derived values for the CRL 618 source size. Pardo et al. (2007) found torus and circumstellar shell sizes of 1.5″ and 3.0″–4.5″, respectively, while millimeter interferometric observations with a ∼5″ beam gave source sizes ≤ 10″ for molecules expected to trace the extended envelope (Remijan et al. 2005). A molecule such as *o*-C_6H_4 is likely to be present in the torus where higher densities shield it from photodissociation, but such a species could also be present in more extended regions if readily formed by ion-molecule chemistry. The GBT beam is ≥ 16″, and so our observations probed both the torus and the extended envelope of CRL 618. A source size of 10″ was assumed for the upper limit calculations, as this includes the entire molecular envelope and therefore all possible regions of emission.

As is shown in Table 1, the most strict *o*-C_6H_4 column density upper limit determined from these observations is 8.4×10^{13} cm^{-2}. The observed benzene column density is 5×10^{15} cm^{-2} (Cernicharo et al. 2001a), and McMahon et al. (2003) report a C_6H_5 column density upper limit in CRL 618 of 4×10^{15} cm^{-2}. The *o*-C_6H_4 upper limit is therefore much lower than the limits for the related species. Given the incomplete nature of the chemical models, however, the significance of this limit is unclear.

Further interpretation of this limit will require additional observational and modeling studies, as this work highlights the nearly total lack of information regarding the physical and chemical properties relevant to benzene-related chemistry in circumstellar environments. Interferometric observations would prove quite useful, as such studies would probe the spatial distribution of molecules in the torus and extended envelope, eliminating the uncertainty in beam dilution effects. Laboratory measurements of the millimeter and submillimeter spectra of *o*-C_6H_4 would aid these observations. We also strongly encourage complete revision of existing PPN models to investigate both the radical- and ion-based benzene chemical networks for comparison to *o*-C_6H_4, C_6H_5, and C_6H_6 observations. Only a combination of further observations, modeling, and laboratory measurements of benzene derivatives will lead to full understanding of PAH formation mechanisms in PPNe.

We would like to thank the NRAO and the GBT support staff, especially Carl Bignell. Support for S. L. W. W. and B. J. M. was provided by an NSF CAREER award (NSF CHE-0449592) and the UIUC Critical Research Initiative program. Support for R. J. M. was provided by NSF-0412707. We are grateful to Matthew Redman and Paul Woods for providing additional details about their chemical models. We would also like to thank Michael Remijan for programming support and development.

REFERENCES

Brown, R. D., Godfrey, P. D., & Rodler, M. 1986, J. Am. Chem. Soc., 108, 1296
Cernicharo, J., et al. 2001a, ApJ, 546, L123
———. 2001b, ApJ, 546, L127
Cherchneff, I., Barker, J. R., & Tielens, A. G. G. M. 1992, ApJ, 401, 269
Frenklach, M., & Feigelson, E. D. 1989, ApJ, 341, 372
Hollis, J. M., Jewell, P. R., Remijan, A. J., & Lovas, F. J. 2007, ApJ, 660, L125
Kraka, E., & Cremer, D. 1993, Chem. Phys. Lett., 216, 333
Kukolich, S. G., Tanjaroon, C., McCarthy, M. C., & Thaddeus, P. 2003, J. Chem. Phys., 119, 4353
McMahon, R. J., McCarthy, M. C., Gottlieb, C. A., Dudek, J. B., Stanton, J. F., & Thaddeus, P. 2003, ApJ, 590, L61
Mebel, A. M., Lin, M. C., Chakraborty, D., Park, J., Lin, S. H., & Lee, Y. T. 2001, J. Chem. Phys., 114, 8421
Müller, H. S. P., Schlöder, F., Stutzki, J., & Winnewisser, G. 2005, J. Mol. Struct., 742, 215
Nummelin, A., Dickens, J. E., Bergman, P., Hjalmarson, Å., Irvine, W. M., Ikeda, M., & Ohishi, M. 1998, A&A, 337, 275
Pardo, J. R., Cernicharo, J., Goicoechea, J. R., Guélin, M., & Ramos, A. A. 2007, ApJ, 661, 250
Redman, M. P., Viti, S., Cau, P., & Williams, D. A. 2003, MNRAS, 345, 1291
Remijan, A. J., Wyrowski, F., Friedel, D. N., Meier, D. S., & Snyder, L. E. 2005, ApJ, 626, 233
Robertson, E. G., Godfrey, P. D., & McNaughton, D. 2003, J. Mol. Spectrosc., 217, 123
Ruze, J. 1966, Proc. IEEE, 54, 633
Sánchez Contreras, C., & Sahai, R. 2004, ApJ, 602, 960
Sarre, P. J. 2006, J. Mol. Spectrosc., 238, 1
Trammell, S. R. 2000, in ASP Conf. Ser. 199, Asymmetrical Planetary Nebulae II: From Origins to Microstructures, ed. J. Kastner, N. Soker, & S. Rappaport (San Francisco: ASP), 147
Ulich, B. L., & Haas, R. W. 1976, ApJS, 30, 247
Woods, P. M., Millar, T. J., Herbst, E., & Zijlstra, A. A. 2003, A&A, 402, 189